ELSEVIER

Check for updates

Fluid eddy induced piezo-promoted photodegradation of organic dye pollutants in wastewater on ZnO nanorod arrays/3D Ni foam

Xiangyu Chen [2,†], Longfei Liu [1,†], Yawei Feng [1], Longfei Wang [2], Zhenfeng Bian [1,*], Hexing Li [1,*], Zhong Lin Wang [2,3,*]

[1] Education Ministry Key and International Joint Lab of Resource Chemistry and Shanghai Key Lab of Rare Earth Functional Materials, Shanghai Normal University, Shanghai 200234, PR China
[2] Beijing Institute of Nanoenergy and Nanosystems, Chinese Academy of Sciences, Beijing 100083, PR China
[3] School of Materials Science and Engineering, Georgia Institute of Technology, Atlanta, GA 30332, USA

A novel nanocomposite with ZnO nanorod arrays vertically growing on the three-dimensional (3D) Ni foam has been synthesized under hydrothermal conditions, which displays both the piezoelectric and photocatalytic functions. When the solution is stirred by magnetic rotation, fluid eddies are produced within the unique macroporous structure in 3D network, causing deformation of ZnO nanorod to generate piezoelectric field. Meanwhile, UV light irradiation on ZnO semiconductor generates photoelectrons and holes, followed by starting photocatalytic degradation of organic dye pollutants in wastewater. The piezo-induced bias voltage promotes the separation of photoelectrons and holes and thus can inhibit their recombination, leading to the enhanced quantum efficiency (more than 5 times). The photocatalytic activity increased by increasing the stirring rate owing to the enhanced piezoelectric field.

Introduction

Environment and energy are two important issues related to the living and daily production of human being. Photocatalysis is a kind of green technology that uses solar energy to generate photoelectrons and holes which further react to produce H_2 and O_2 *via* water splitting, to induce CO_2 conversion, to reduce heavy metallic ions, and to degrade organic pollutants [1–6]. Accordingly, photocatalysis using sustainable solar energy has great potential in the fields of energy and environment. So far, the most important factor affecting the photocatalytic performance is the photoelectron–hole recombination [3–4,6]. To date, great efforts have been made in order to prevent the recombination. Previous studies have shown that metal or nonmetal ion doping, noble metal modification, heterojunction structure formation, and unique nanostructure fabrication can promote the photo-generated electron and hole separation [5,7–19]. Meanwhile, photoelectrocatalysis is also an effective technique to suppress photoelectron–hole recombination by the bias electric field [20–22]. However, the application of this process is quite limited since it requires the external bias voltage, the electrode coated with photocatalyst, and the electrolytes in liquid phase reaction. Moreover, the photocatalyst coated on the electrode may greatly reduce the effective surface area, corresponding to the decreased light absorption and active site number.

Recently, ZnO has received considerable attention because of its excellent photocatalytic and piezoelectric properties [23–27]. When the c-axis of ZnO microrod or nanorod is applied deformation, a piezoelectric field can be created on the surface [28–30]. This built-in electric fields from piezoelectric materials can be applied to separate photoelectron and holes, leading to the decreased recombination rate and thus the enhanced photocatalytic activity [31–41].

Up to now, the production of build-in electric field of ZnO has been realized by several methods. The strong external force is applied to form the piezoelectric field in ZnO nanostructures.

* Corresponding authors at: School of Materials Science and Engineering, Georgia Institute of Technology, Atlanta, GA 30332, USA (Z.L. Wang).
E-mail addresses: Bian, Z. (bianzhenfeng@shnu.edu.cn), Li, H. (hexing-li@shnu.edu.cn), Wang, Z.L. (zlwang@gatech.edu).
† These authors contributed equally to this work.

1369-7021/© 2017 Elsevier Ltd. All rights reserved. https://doi.org/10.1016/j.mattod.2017.08.027

Ultrasonic wave or friction is also employed to produce the high piezoelectric effect by the applied deformation of ZnO nanomaterials [34,38,40–41]. However, there are still various forms of mechanical energy in the natural environment, such as water flow, wind, and tide, which cannot be easily utilized in the piezo-enhanced photocatalytic process. Taking into account the potential applications of photocatalysis in cleaning water and air, the flow or wind driven piezo-promoted photocatalysis will offer more opportunities for the practical applications.

Herein, we report for the first time the piezo-promoted photocatalysis with enhanced activity in degradation of organic pollutants in wastewater by using ZnO nanorod arrays vertically grown on the three-dimensional (3D) structure Ni foam substrate. The water flow induced by stirring generate piezoelectric field of the ZnO arrays and the intensity increased with the increase in stirring rate. Meanwhile, the 3D porous structure can enhance the piezoelectric field owing to some small water turbulences on the inner surface of the Ni foam. More importantly, such 3D structure is more effective in reactant-diffusion and photocharge-migration, leading to the enhanced photocatalytic activity.

Results and discussion

As shown in Fig. 1a, the Ni substrate shows a typical macroporous foam-like structure with three dimensional network (3D) with a large range of pore-size distribution. The high-resolution SEM image (Fig. 1b) displays smooth surface of Ni foam skeleton owing to the close package of nickel particles. Fig. 1c shows that ZnO nanorod arrays are uniformly deposited on the surface of Ni foam. The high-resolution SEM image (Fig. 1d) indicates that the ZnO nanorod arrays are vertically grown on the surface of the Ni foam. According to the attached side-view SEM image, the length and the diameter of ZnO nanorods are determined around 1 μm and 50 nm, respectively.

The XRD patterns in Fig. 2 display strong diffraction peaks characteristic of metallic Ni in both the pure Ni foam and the ZnO nanorod arrays/Ni foam. Very weak diffraction peaks indicative of ZnO could be found in the ZnO nanorod arrays/Ni foam, corresponding to the hexagonal wurtzite structure of ZnO crystals (JCPDS 36-1451) [34–35,38,40]. No other impurity peaks are observed, suggesting the formation of well-defined nanocomposite in the form of ZnO nanorod arrays/Ni foam.

The separation efficiency of photogenerated charges is one of the most important factors determining photocatalytic activity, which could be examined by the transient photocurrent density. As shown in Fig. 3, the photocurrent of the ZnO nanorod arrays/Ni foam generated at 500 rpm stirring rate is about 10 μA/cm^2, which is much higher than that obtained at static condition (0 rpm). This means that the migration of photogenerated charges in ZnO nanorod arrays is much easier due to the presence of piezoelectric field resulting from water-stirring. With the increase in stirring rate to 1000 rpm, the photocurrent density also increases. One possible reason is that the swirl of water flow produces a mechanical force to the top of ZnO nanorod arrays during the stirring process, resulting in the ZnO nanorod

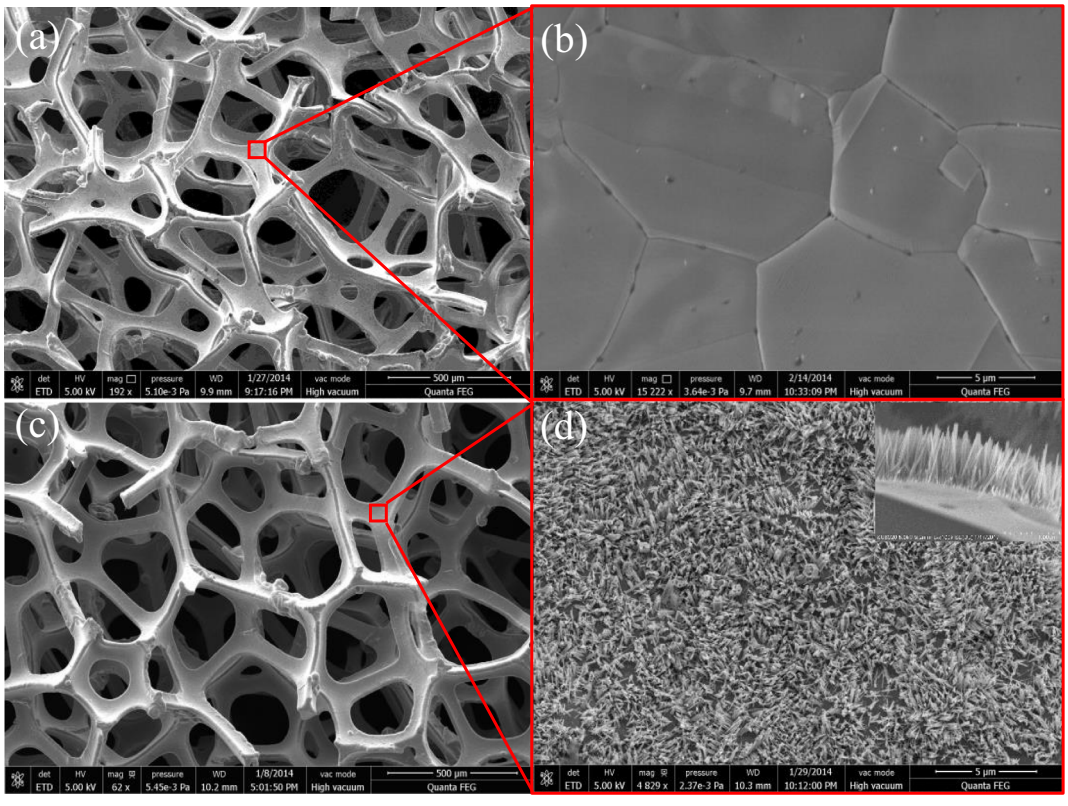

FIGURE 1

Scanning electron microscopy (SEM) image (a) and high-resolution SEM image (b) of Ni foam. SEM image (c) and high-resolution SEM image (d) of ZnO nanorod arrays/Ni foam. The inset is the side-view SEM image.

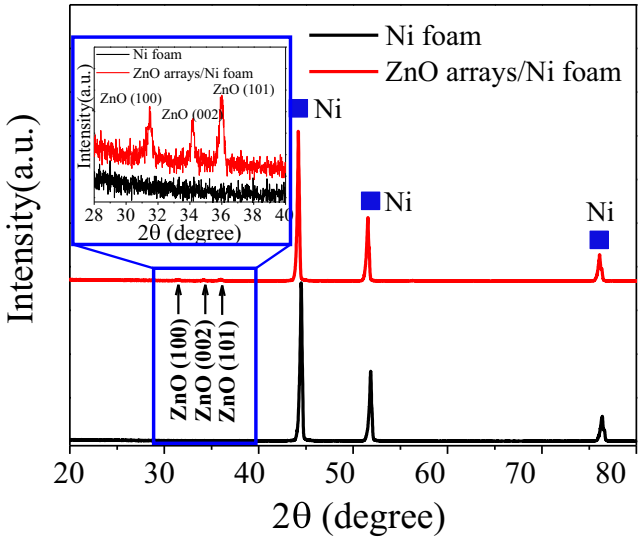

FIGURE 2

X-ray diffraction (XRD) patterns of Ni foam and ZnO nanorod arrays/Ni foam.

deformation to generate a piezoelectric field (Fig. 4) [29,30]. With the increase in stirring rate, the water flow velocity also increases, corresponding to the enhanced interaction force between the Ni foam and water flow. Meanwhile, the ZnO nanorod on the surface of Ni foam also experiences an enhanced mechanical force, which may induce the enhanced deformation degree. The increased piezo can promote the photo-charges separation (as can be seen in Fig. 4), which can inhibit photoelectron–hole recombination. Therefore, the ZnO nanorod arrays/Ni foam displays increasing photocurrent with the increase in stirring rate.

Fig. 5 shows the activity of ZnO nanorod arrays/Ni foam during UV light driven photocatalytic degradation of rhodamine B (RhB) at different stirring rate. The RhB degradation efficiency reaches 35% after 90 min without stirring (stirring rate = 0 rpm), corresponding to the reaction rate of 0.005 min^{-1}. The degradation efficiency gradually increases to 92% with the stirring rate increasing to 1000 rpm, corresponding to the increase in reaction rate up to 0.026 min^{-1}, which is about 5 times as that obtained without stirring. The reaction rate increases almost linearly with the stirring rate (Supplementary Fig. S1), showing the promoting

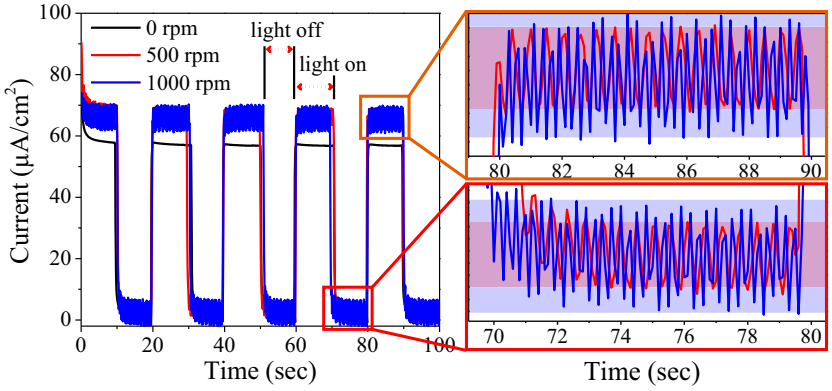

FIGURE 3

UV light (365 nm) induced photocurrent pulse-curves of ZnO nanorod arrays/Ni foam at different stirring rate.

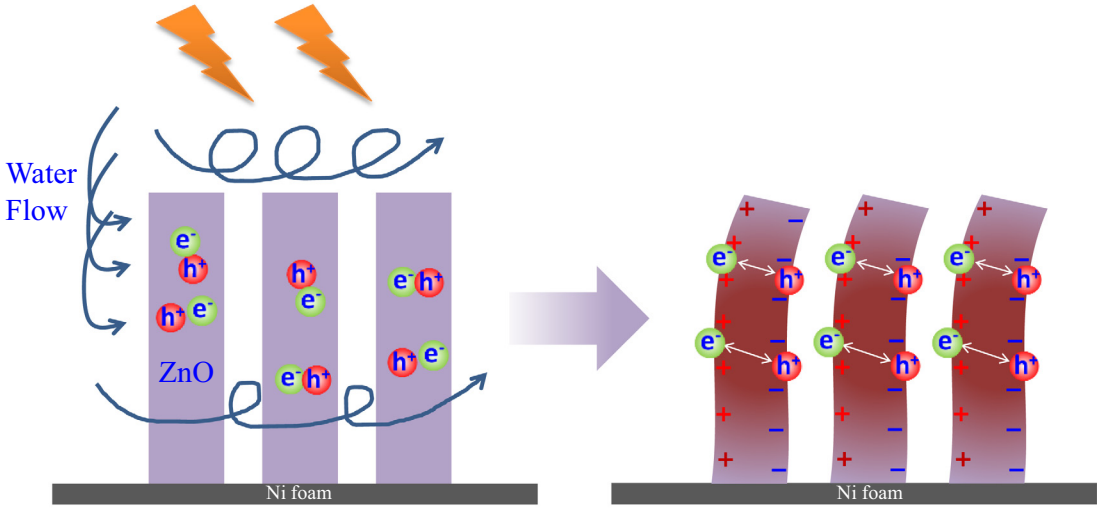

FIGURE 4

Schematic illustration of the formation of piezoelectric field due to ZnO nanorod deformation caused by the water flow and turbulence during stirring and the piezo-promoted separation of photoelectrons from holes in ZnO nanorod arrays/Ni foam.

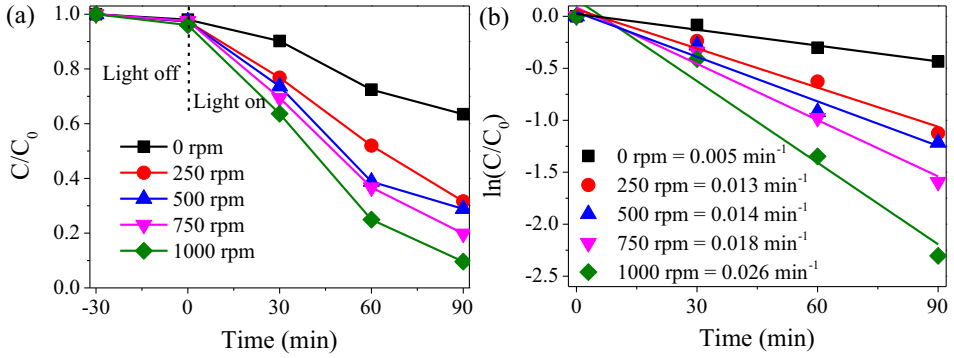

FIGURE 5

Photocatalytic degradation of RhB on ZnO nanorod arrays/Ni foam at different stirring rate under UV light irradiation. (a) Degradation yield and (b) kinetic linear fitting curve with the reaction time. Reaction conditions: 20 mL RhB (5.0 mg/L), Xe lamp (365 nm, 100 W), reaction temperature = 298 K.

effect of the piezo on photocatalysis since it can facilitate the separation of photoelectrons from holes to inhibit their recombination. With the increase in stirring rate, the piezoelectric field becomes stronger, which can further promote the separation of photoelectrons from holes, leading to the enhanced photocatalytic activity. More importantly, the ZnO nanorod arrays/Ni foam can be easily recycled and used repetitively for more than 5 times without significant deactivation, indicating the excellent durability (Supplementary Fig. S2).

To further confirm the promoting effect of piezoelectric field on photocatalysis, we prepare a reference nanocomposite with ZnO nanoparticles instead of ZnO nanorod arrays growing on the Ni foam substrate. The SEM images (Fig. S3) display uniform dispersion pf ZnO nanoparticles on the surface of Ni foam with diameter around 100 nm. Similar to that in the ZnO nanorod arrays/Ni foam, the ZnO in the ZnO nanoparticles/Ni foam is also present in the hexagonal wurtzite structure (see the XRD pattern in Supplementary S4). As shown in Fig. 6, the ZnO nanoparticles/Ni foam exhibits 21% RhB degradation yield after 90 min photocatalytic reaction under UV light irradiation at stirring rate of 0 rpm, which is slightly lower than the ZnO nanorod arrays/Ni foam. Since the ZnO nanorod arrays display lower surface area than the ZnO nanoparticles, we conclude that the enhanced light absorbance resulting from the multiple light reflections within well-arranged ZnO nanorod arrays can account for the higher photocatalytic activity of the ZnO nanorod arrays/Ni foam.[6, 16] In contrast to the ZnO nanorod arrays/Ni foam, the ZnO nanoparticles/Ni foam does not show significant influence of stirring rate on the photocatalytic activity. Obviously, the deformation of ZnO nanoparticles under the external mechanical force is much more difficult than the ZnO nanorod arrays due to the strong interaction between ZnO nanoparticles and Ni foam substrate. Therefore, the piezoelectric field generated in the ZnO nanoparticles/Ni foam is not enough to drive the separation of photoelectrons from holes, which could sufficiently account for the little or even no promoting effect on the photocatalytic activity for degrading RhB by applying stirring in the wastewater.

The photocatalytic performances of ZnO nanorod arrays/ITO and ZnO nanorod arrays/glass are also examined to show the role played by 3D Ni foam substrate in the ZnO nanorod arrays/Ni foam In those two nanocomposites, the ZnO nanorods also vertically and uniformly grow on the surface of ITO and glass substrates with length around 1 μm and 0.6 μm, respectively (see Supplementary Figs. S5 and S6). As shown in Fig. 7, the ZnO

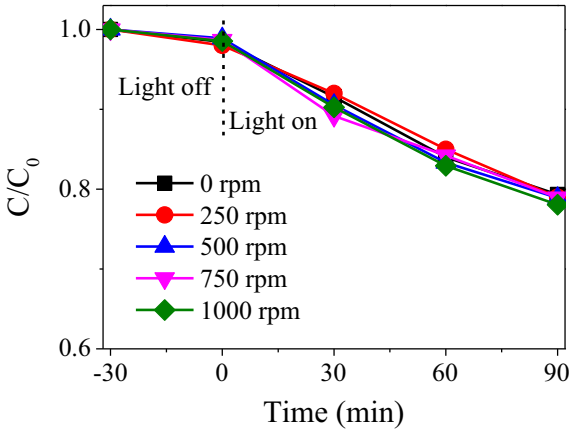

FIGURE 6

Photocatalytic degradation of RhB on ZnO nanoparticles/Ni foam at different stirring rate under UV light irradiation. Reaction conditions are given in Fig. 5.

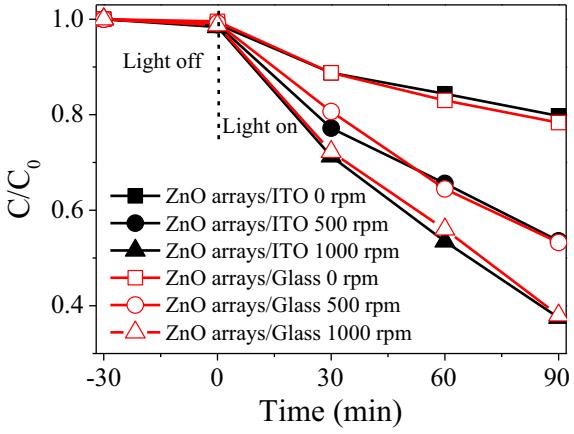

FIGURE 7

Photocatalytic degradation of RhB on ZnO nanorod arrays/ITO and ZnO nanorod arrays/glass at different stirring rate under UV light irradiation. Reaction conditions are given in Fig. 5.

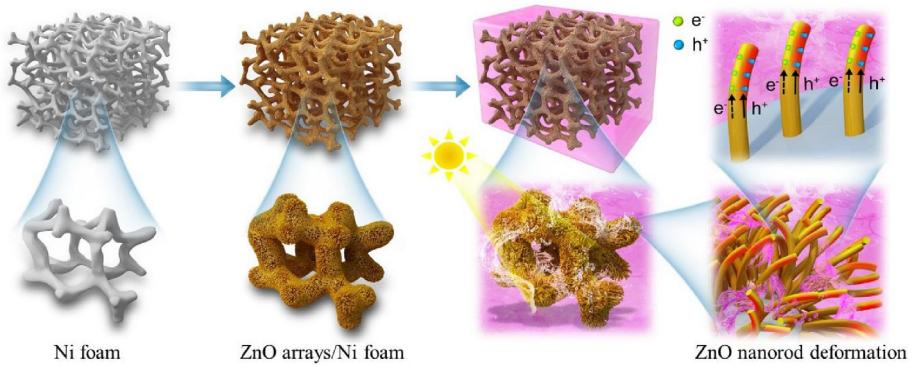

FIGURE 8

Synergetic effects between piezoelectric field and photocatalysis of ZnO nanorod arrays/Ni foam.

nanorod arrays/ITO exhibits almost the same photocatalytic activity and the same effect of stirring rate as the ZnO nanorod arrays/glass. Taking into account that the ITO is a good electric conductor while the common glass is an electric insulator, we therefore conclude that electric conductivity of the substrate has very little or no influence on either the photocatalytic or the piezoelectric performances of ZnO nanorod arrays. Comparing Fig. 7 with Fig. 5, we found that, under the same reaction conditions, the RhB degradation yield on either the ZnO nanorod arrays/ITO or the ZnO nanorod arrays/glass is significantly lower than that on the ZnO nanorod arrays/Ni foam. This could be mainly attributed to the unique 3D structure which could increase the dispersion degree of ZnO nanorod arrays and also facilitate the reactant-diffusion. Interestingly, when the stirring rate increases from 0 rpm to 1000 rpm, both the RhB degradation yield and photocatalytic reaction rate increase by about 3 times on the ZnO nanorod arrays/ITO (see Fig. 7 and Supplementary Fig. S7). However, those observed on the ZnO nanorod arrays/Ni foam increase by about 5 times (see Fig. 5). This could be accounted by considering the unique 3D structure of the Ni foam substrate, in which more flow turbulence or eddies can be generated during stirring, leading to the enhanced piezoelectric effect and thus the enhanced photocatalytic activity.

Fig. 8 schematically illustrates the synergetic effects between piezoelectric field and photocatalysis of the ZnO/Ni nanocomposite. Firstly, ZnO nanorod arrays are vertically grown on the Ni foam *via* a simple hydrothermal treatment. The ZnO serves as both the piezoelectric and the photocatalytic material. On one hand, the macroporous structure with 3D network of the ZnO nanorod arrays/Ni foam allows good liquid flow to produce turbulence or eddy by stirring solution, which induces piezoelectric field owing to the deformation ZnO nanorod arrays. On the other hand, the UV light irradiation onto ZnO semiconductor induces photoelectrons and holes on valence and conduction bands, followed by starting the photocatalytic degradation of organic dye pollutants like RhB in wastewater directly or *via* forming other active radicals like superoxide radicals and hydroxyl radicals . Inhibition of photoelectron–hole recombination plays a key role in determining the quantum efficiency. By stirring the solution, a large number of turbulences and eddies are produced within the ZnO/Ni interface owing to the unique macroporous structure with 3D network, which causes deformation of ZnO nanorod to generate piezoelectric field. The piezo-induced bias voltage promotes the photoelectron transfer through Ni conductor, which favors the separation of photoelectrons from holes to inhibit their recombination, leading to the enhanced photocatalytic activity. The photocatalytic activity increased with the increase in stirring rate owing to the enhanced piezoelectric field.

Conclusions

This work develops a novel piezo-promoted photocatalysis for degradation of organic pollutants like RhB in wastewater by using a nanocomposite with ZnO nanorod arrays vertically growing onto the 3D Ni foam. Piezoelectric field is generated owing to the deformation of ZnO nanorod caused by flow turbulence and eddy within macroporous structure of 3D network generated by stirring the solution. Meanwhile, the ZnO generates photoelectrons and holes under UV light irradiation, followed by starting photocatalysis. The piezo-induced bias voltage promotes the separation of photoelectrons from holes, leading to the low photoelectron–hole recombination rate and high photocatalytic activity. The 3D network of Ni foam substrate plays a key role in promoting photocatalysis owing to the enhanced piezoelectric field and diminished diffusion limit. The photocatalytic activity increases with the increase in stirring rate owing to the enhanced piezoelectric field. This work supplies a new way to design efficient photocatalysts which may offer more opportunities for practical applications in wastewater cleaning.

Experimental section

Reagents

Zinc nitrate hexahydrate (99%, metals basis), hexamethylenetetramine (99 + %), rhodamine B (RhB) are purchased from Alfa Aesar. Ni foam (thickness = 1.5 mm, surface density = 320, size = 35 mm × 25 mm) is purchased from Changde Liyuan Co., Ltd. ITO glass is purchased from Suzhou Jinggui Technology Co., Ltd. Common glass is got from the microscope slides (SAIL Brand). All the reagents are used without further purification. Solutions are prepared with deionized water.

Sample preparation

In a typical process, the ZnO nanorod arrays/Ni foam is synthesized by seed-assisted hydrothermal method [42]. The Ni foam is firstly cleaned by ultrasonication for 15 min in ethanol and deionized water, followed by drying at 60 °C overnight. The ZnO seed layer (Ar, 100 W, 15 min) is then deposited on the Ni foam substrate by radio frequency (RF) magnetron sputtering at room temperature (Denton Vacuum/Discovery 635), followed by immersing into 80 mL aqueous solution containing 0.015 mol/L Zinc nitrate hexahydrate and 0.02 mol/L hexamethylenetetramine at 90 °C for 6 h. Finally, the solid product is washed thoroughly with alcohol and deionized water, and dried at 70 °C. For comparison, the ZnO nanorod arrays/ITO and the ZnO nanorod arrays/glass are also synthesized in the same way by using ZnO nanorod arrays/ITO and the ZnO nanorod arrays/glass. The reference sample (ZnO nanoparticles/Ni foam) was prepared by sputtering deposition for 2 h.

Characterizations

The as-received samples were characterized using X-ray diffraction (XRD, PANalytical X'Pert^3 Powder, CuKα source), scanning electron microscopy (SEM, HITACHI SU8020). The photocurrent characteristics of the device were recorded by an electrochemical workstation (CHI660E).

Activity test

The photocatalytic degradation of RhB in an aqueous solution (5.0 mg/L) is started by irradiating with 365 nm UV light (100 W) after being stirred in dark for 30 min to reach absorption–desorption equilibrium. During the reactions, the stirring rate is adjusted at 0, 250, 500, 750 or 1000 rpm to achieve different piezo-induced bias voltage. The RhB concentration is analyzed by a UV spectrophotometer (UV3600) at their characteristic wavelength (554 nm) to determine the degradation yield.

Photoelectrochemical (PEC) measurement

Photoelectrochemical measurement is performed by using an electrochemical station (CHI 660E). The nanocomposite of ZnO nanorod arrays/Ni foam serves as a working electrode. The counter electrode and reference electrode are consisted of a Pt sheet (99.99%, 0.1 mm, 2 cm * 2 cm) and saturated calomel electrode (SCE), respectively. A 100 W Xe lamp with 365 nm wavelength is positioned at 8 cm away from the photoelectrochemical cell. The photocurrent is measured in a 0.5 mol/L Na_2SO_4 solution using a 10 s on–off cycle at a bias voltage of 0.5 V.

Acknowledgements

This work is supported by National Natural Science Foundation of China (Grant No. 21237003, 21407106, 21522703, 21377088, 51432005, 5151101243, 51561145021), Shanghai Government (14ZR1430800, 13SG44, 15520711300), and International Joint Laboratory on Resource Chemistry (IJLRC), the National Key R & D Project from Minister of Science and Technology (2016YFA0202704), Beijing Municipal Science & Technology Commission (Y3993113DF). Research is also supported by The Program for Professor of Special Appointment (Eastern Scholar) at Shanghai Institutions of Higher Learning and the Ministry of Education of China (PCSIRT_IRT_16R49).

Appendix A. Supplementary data

Supplementary data associated with this article can be found, in the online version, at http://dx.doi.org/10.1016/j.mattod.2017.08.027.

References

[1] A. Kudo, Y. Miseki, Chem. Soc. Rev. 38 (2009) 253–278.
[2] A.J. Morris, G.J. Meyer, Acc. Chem. Res. 42 (2009) 1983–1994.
[3] J.G. Yu et al., J. Am. Chem. Soc. 136 (2014) 8839–8842.
[4] H. Tong et al., Adv. Mater. 24 (2012) 229–251.
[5] H. Wang et al., Chem. Soc. Rev. 43 (2014) 5234–5244.
[6] Z.F. Bian, J. Zhu, H.X. Li, J. Photochem. Photobiol., C 28 (2016) 72–86.
[7] D. Dvoranova et al., Appl. Catal., B 37 (2002) 91–105.
[8] R. Nakamura, T. Tanaka, Y. Nakato, J. Phys. Chem. B 108 (2004) 10617–10620.
[9] T. Ohno et al., Appl. Catal., A 265 (2004) 115–121.
[10] A.W. Xu, Y. Gao, H.Q. Liu, J. Catal. 207 (2002) 151–157.
[11] S. Linic, P. Christopher, D.B. Ingram, Nat. Mater. 10 (2011) 911–921.
[12] V. Subramanian, E. Wolf, P.V. Kamat, J. Phys. Chem. B 105 (2001) 11439–11446.
[13] Z.F. Bian et al., J. Phys. Chem. C 116 (2012) 25444–25453.
[14] Z.F. Bian, T. Tachikawa, T. Majima, J. Phys. Chem. Lett. 3 (2012) 1422–1427.
[15] Z.F. Bian et al., J. Am. Chem. Soc. 136 (2014) 458–465.
[16] Z.F. Bian et al., J. Am. Chem. Soc. 134 (2012) 2325–2331.
[17] F.F. Chen et al., Langmuir 31 (2015) 3494–3499.
[18] C. Tang et al., Appl. Catal., B 201 (2017) 41–47.
[19] Y. Ma et al., Chem. Rev. 114 (2014) 9987–10043.
[20] F.E. Osterloh, Chem. Soc. Rev. 42 (2013) 2294–2320.
[21] A. Paracchino et al., Nat. Mater. 10 (2011) 456–461.
[22] J.H. Yang et al., Acc. Chem. Res. 46 (2013) 1900–1909.
[23] Z.R. Tian et al., Nat. Mater. 2 (2003) 821–826.
[24] Z.L. Wang, ACS Nano 2 (2008) 1987–1992.
[25] S. Xu, Z.L. Wang, Nano Res. 4 (2011) 1013–1098.
[26] P. Yang et al., ACS Nano 7 (2013) 2617–2626.
[27] Q. Zhang et al., Adv. Mater. 21 (2009) 4087–4108.
[28] X. Han et al., Adv. Mater. 21 (2009) 4937–4941.
[29] W.L. Hughes, Z.L. Wang, J. Am. Chem. Soc. 126 (2004) 6703–6709.
[30] G. Mantini, Y. Gao, Z.L. Wang, Nano Res. 2 (2009) 624–629.
[31] D. Hong et al., Mater. Interfaces 8 (2016) 21302–21314.
[32] S. Li et al., J. Phys. Chem. C 114 (2010) 2903–2908.
[33] C.F. Tan, W.L. Ong, G.W. Ho, ACS Nano 9 (2015) 7661–7670.
[34] L. Wang et al., ACS Nano 10 (2016) 2636–2643.
[35] Z.L. Wang, Chin. Sci. Bull. 54 (2009) 4021–4034.
[36] X.Y. Chen et al., Adv. Funct. Mater. 27 (2017) 1603788.
[37] X.Y. Chen et al., Adv. Funct. Mater. 26 (2016) 4906–4913.
[38] H. He et al., Nano Energy 31 (2017) 37–48.
[39] J.H. Lin et al., Nano Energy 31 (2017) 575–581.
[40] X.Y. Xue et al., Nano Energy 13 (2015) 414–422.
[41] K.S. Hong et al., J. Phys. Chem. C 116 (2012) 13045–13051.
[42] L.P. Zhu et al., Adv. Sci. 4 (2017) 1600185.